Fluid Dynamics and Co-located Conferences
June 24-27, 2013, San Diego, CA
31st AIAA Applied Aerodynamics Conference
31st AIAA Applied Aerodynamics Conference: Low speed, low Reynolds number aerodynamics

Design of a 2-D Fairing for a Wind Turbine Tower

Kyle O'Connor*, Eric Loth†
University of Virginia, Charlottesville, VA, 22904

Michael S. Selig‡
University of Illinois at Urbana-Champaign, Urbana, IL, 61801

An aerodynamic shroud was designed to reduce the effects of the wind turbine tower wake on the blades of a downwind rotor. For a given tower diameter and wind speed the shroud was designed to have the minimum drag and minimum chord length downstream of tower centerline, while being able to self-align and resist flow separation when subjected to a non-zero angle of attack. The initial analysis was run using XFOIL and showed that a three-to-one chord-to-thickness ratio resulted in the minimum drag. Based on this result, the NACA0033 airfoil was selected as the baseline. Further analysis showed that a shroud of this shape will not self-align due to the tower center being located behind the aerodynamic center. A new series of airfoils was created to have a 33% thickness ratio starting from a NACA0028, NACA0030, and NACA0031. The resulting airfoils all had significant adverse pressure gradients near their maximum thickness locations that could lead to flow separation. A new group of airfoils were created by adjusting the existing airfoil geometry using PROFOIL. Of the 13 airfoil designs that were analyzed, the C30u design had the best overall performance and met all of the objectives. At a Reynolds number based on tower diameter of 8.3×10^6, the C30u design had a drag coefficient based on inscribed tower diameter of 0.0193, which represents a 97.5% reduction in the drag of the cylinder. At a 5 degree angle of attack, the C30u design had a pitching moment coefficient of -0.0128.

Nomenclature

α	=	angle of attack
c	=	chord length
C_d	=	2-D drag coefficient based on chord
$C_{d,D}$	=	2-D drag coefficient based on tower diameter
C_m	=	2-D moment coefficient
$C_{m\alpha,D}$	=	change in the 2-D moment coefficient about the inscribed cylinder center with respect to angle of attack
C_p	=	pressure coefficient
D	=	tower diameter
F_d'	=	2-D drag force per unit length
ρ	=	density
Re	=	Reynolds number based on chord
Re_D	=	Reynolds number based on tower diameter
t	=	thickness
V	=	freestream flow velocity
x	=	location along the airfoil chord line
x_D	=	x/c location of tower center
x_t	=	x/c location of airfoil maximum thickness
x_{TE}	=	x/c location of trailing edge ($x_{TE} = 1$)

* Graduate Researcher, Mechanical and Aerospace Engineering, 122 Engineer's Way, AIAA Member
† Professor, Mechanical and Aerospace Engineering, 122 Engineer's Way, AIAA Associate Fellow
‡ Associate Professor, Aerospace Engineering, 104 S. Wright St., AIAA Senior Member

I. Introduction

A. Motivation for Shroud

The average wind turbine rated power has increased twenty-fold since 1985 with present large-scale systems greater than 5 MW. Future extreme-scale systems with power levels of 20 MW will have rotor diameters on the order of 240 m. These future "extreme-scale" (10+ MW) systems will be difficult to construct with conventional rotor geometries due to the combination of the stiffness constraints and increases in blade mass. The rotor cost is proportional to mass, and the rotor accounts for a significant amount of the initial total system cost, with many other turbine components increasing in scale and cost as the rotor mass increases. Thus, new concepts in turbine blade design are needed to decrease the mass.

Conventional upwind turbine configurations, like the one shown in Fig. 1a, typically employ blades with fiberglass shells to carry the structural and aerodynamic loads with small aeroelastic deflection to avoid tower strikes and fatigue. The designed stiffness to avoid tower strikes and fatigue leads to the blade mass problems discussed above. This stiffness constraint can be relaxed if a downwind morphing concept is employed so that the blade mass can be reduced, which leads to a reduction in cost. The potential to reduce the cost means that new large designs are more likely to have a downwind rotor. A segmented ultralight morphing rotor (SUMR) design was proposed by Loth et al.[1] to allow for the manufacture of extreme-scale turbines. A conceptual image of the SUMR design is shown in Fig. 1b. In this design, the rotor can begin to morph as the wind speeds increase and then fully-align with the resultant forces when wind speeds are high. The vast majority of stress-inducing cantilever loads on a conventional upwind rotor are due to downwind moments. The forces can combine to induce significant cantilever loads in the downwind direction for a conventional blade. However, if the forces are aligned along the blade, the structural loads are reduced to primarily acting in tension, which drastically reduces stresses for a given structure. This aligning is especially important for extreme-scale systems for which the downwind cantilever forces and gravity stresses rapidly increase blade masses. The downstream angle needed for alignment increases with turbine rated power, making the morphing concept more attractive, especially for 10 MW and higher systems.[2] Initial tests showed that this method allows for a 50% reduction in blade mass compared to a conventional blade.[3]

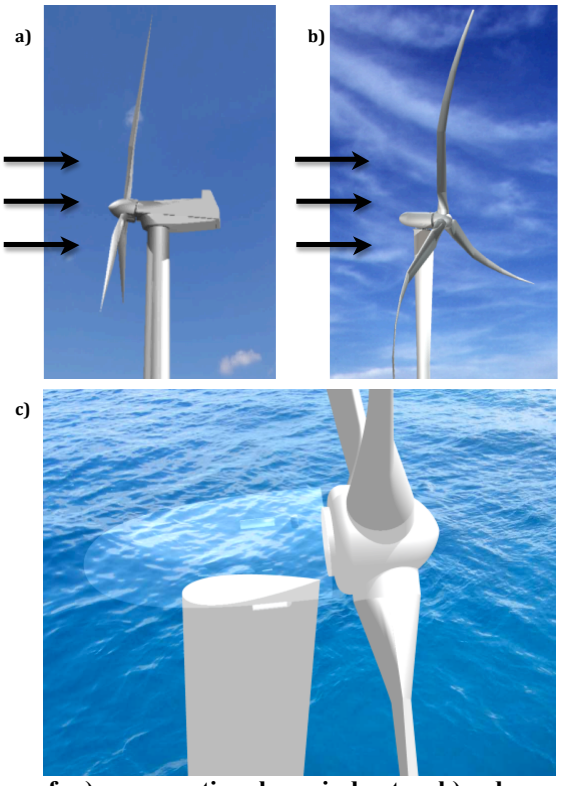

Figure 1. Conceptual images of: a) a conventional upwind rotor, b) a downwind morphing rotor, and c) an aerodynamically faired tower for reduced tower wake effects (from Loth et al.[2]).

The most common concern about using a downwind rotor is the effect of the tower wake on the downstream blades. When a blade passes through the velocity deficit of the wake, it experiences a change in the relative angle of attack. The sudden change in the aerodynamic loading on the blade can cause the blade to flutter. A wind turbine rotor will typically go through thousands of revolutions a day and millions of revolutions a year. If the blade experiences a slight flutter every revolution, the effects can be compounded, resulting in significant blade fatigue and greatly reducing the life span of the blade. However, employing an aerodynamically faired tower, like the one shown in Fig. 1c, can mitigate these negative effects. Such geometry will have a substantial impact because the drag (and turbulent wake) of an airfoil is many times less than that of a cylinder.

Wind turbines operate in the subsonic regime, therefore the tower influences the flow that the blades experience even for an upwind design. While this design is most significant for downwind turbines, the inclusion of a tower shroud can also be beneficial for upwind designs. This design is even more promising when an entire wind farm is considered instead of a single turbine. The use of a tower shroud can help to reduce the effects of the entire turbine on the freestream velocity, allowing turbines to be packed more closely together while still capturing the same amount of energy, which could potentially lead to a significant increase in the amount of power generated by a wind farm per acre.

B. Previous Studies on Fairings and Shrouds

Many techniques have been implemented in an attempt to reduce the drag of a cylinder. Sang-Joon Lee et al.[4] were able to reduce the drag by 25% by installing a small control rod upstream of the cylinder. Mohammad Mashud et al.[5] also achieved a 25% reduction in drag by attaching circular rings around the cylinder. Sosa, D'Adamo, and Artana[6] were also able to reduce the drag by 25% with the use of three-electrode plasma actuators. Jong-Yeon Hwang and Kyung-Soo Yang[7] were able to achieve greater success in reducing the cylinder drag by nearly 40% by installing one splitter plate upstream of the cylinder and another in the cylinder wake. Finally, Triyogi, Suprayogi, and Spirda[8] were able to reduce the drag of a cylinder by nearly 50% by installing an I-type bluff body upstream of the cylinder. None of these techniques were able to reduce the cylinder drag to a level similar to the drag of a typical airfoil.

The drag of a wind turbine tower can be greatly reduced, by more than 90%, by incorporating an aerodynamically faired shroud around the cylindrical tower, like shown in Fig. 2. Such a shroud would significantly reduce the effects of the tower wake on the rotor blades. One drawback for use with a downwind turbine is that the turbine rotor must be moved further downstream so that the tower would have to be able to support increased cantilever loads.

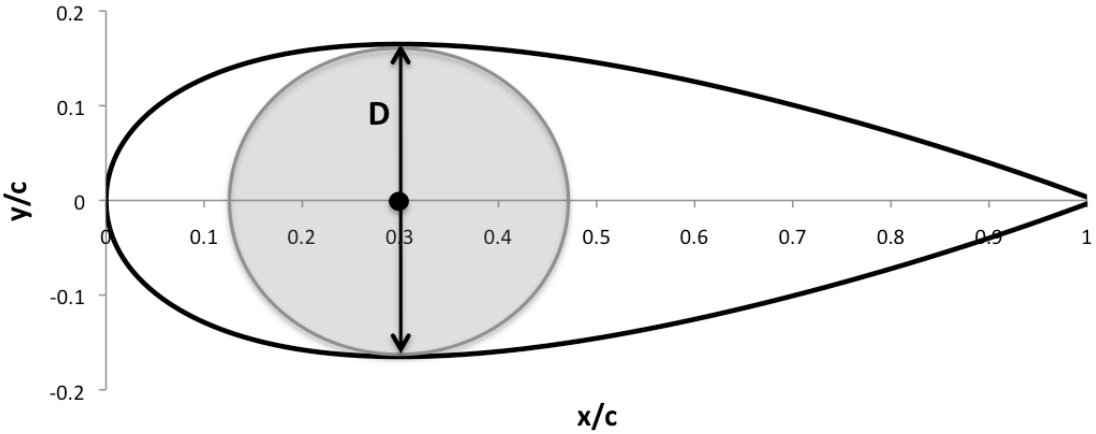

Figure 2. Geometry of the NACA0033 and location of tower cylinder with diameter *D*.

It is clear that a streamlined shroud would have a positive impact on the drag of the turbine tower, though the optimal shroud geometry must be determined. XFOIL, a program for the design and analysis of subsonic airfoils, was used to calculate the drag coefficient of various airfoil shapes. XFOIL provides the drag coefficient based on chord, viz

$$C_d \equiv \frac{F_d'}{\frac{1}{2}\rho V^2 c} \tag{1}$$

For this study we are interested in the drag coefficient based on the diameter of the inscribed cylinder, which is constant based on the diameter of the turbine tower, viz

$$C_{d,D} \equiv \frac{F_d'}{\frac{1}{2}\rho V^2 D} \tag{2}$$

The coefficient of drag that XFOIL provides (Eq. 1) can easily be converted to the drag coefficient based on tower diameter (Eq. 2) by multiplying it by the airfoil chord and dividing by the tower diameter. The drag coefficient will change with the Reynolds number, viz

$$Re \equiv \frac{\rho V c}{\mu} \tag{3}$$

The Reynolds number (Eq. 3) depends on the chord of the airfoil, therefore it is different for each airfoil. The Reynolds number can be converted to a Reynolds number based on tower diameter, which is constant for each airfoil, viz

$$Re_D \equiv \frac{\rho V D}{\mu} \tag{4}$$

The Reynolds number based on tower diameter (Eq. 4) is obtained by multiplying the Reynolds number based on chord (Eq. 3) by the tower diameter and dividing by the airfoil chord.

One important characteristic for the shroud is that it should self-align around its pivot point when the flow approaches at a non-zero angle of attack. To check if the tower is self-aligning, the change in the moment coefficient about the tower center with respect to angle of attack must be calculated, viz

$$C_{m\alpha,D} \equiv \left.\frac{\partial C_m}{\partial \alpha}\right|_{X_D} \tag{5}$$

A self-aligning, passive shroud, i.e. without a shroud yaw drive, will have a negative $C_{m\alpha D}$ value, which means the moment coefficient will be negative at a positive angle of attack and positive at a negative angle of attack.

Figure 3 shows the comparison between the drag coefficients for elliptic airfoils and symmetric NACA airfoils for different chord-to-thickness ratios. The data for the ellipses were taken from Blevins,[9] while the symmetric NACA airfoil data were calculated at different Reynolds numbers using XFOIL. The drag coefficient is lower for symmetric NACA airfoils, even at a lower Reynolds number, which is significant because the drag coefficient typically increases as Reynolds number decreases. Figure 3 also includes data for the reduced cylinder drag from the studies mentioned earlier. Implementing an aerodynamic shroud around the tower is significantly more effective at reducing the drag than any of the other methods.

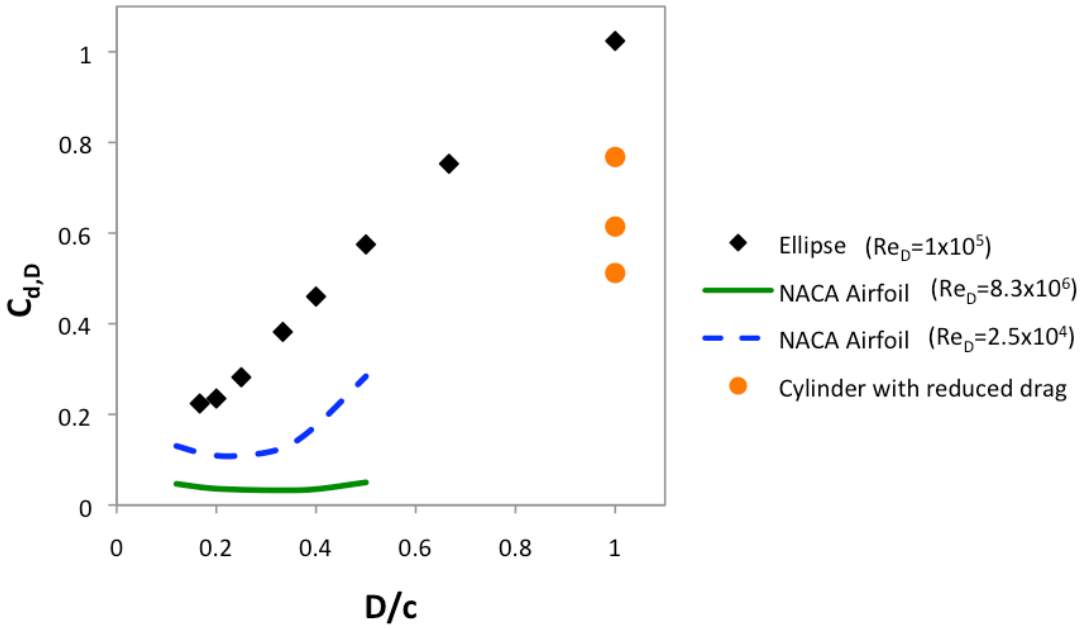

Figure 3. Drag coefficient at zero degree angle of attack for a cylinder, ellipses, and symmetric NACA airfoils ranging from NACA0012 to NACA0050, where D is the maximum circle diameter that can be inscribed in a given shape and c is the streamwise length (ellipse data from Blevins,[9] and reduced drag data from Lee et al.[4], Hwang et al.[7], and Triyogi et al.[8]).

There have not been many experiments done to test how much the wake unsteadiness of a wind turbine can be reduced by using an aerodynamically faired tower, most likely due to the fact that conventional turbines use an upwind design where the tower has little influence on the flow that the rotor sees. During their unsteady aerodynamics testing, Hand et al.[10] did take wake measurements for NREL while using a symmetric airfoil-shaped shroud (0.46 m thickness, 0.89 m chord) in a downwind turbine configuration. Unfortunately the test results are unavailable.

A study at the Masdar Institute of Science and Technology[11] simulated the interaction between the tower and rotor for a downwind design. The simulation was run using a NACA0012 airfoil cross-section and a circular cross-section. The airfoil and circular cross-sections resulted in 5% and 57% reductions in the lift forces on the rotor blade, respectively.

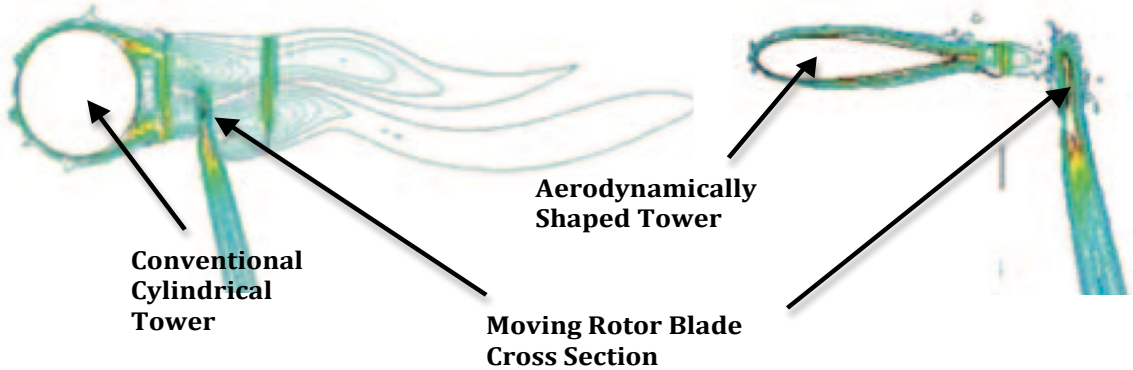

Figure 4. Wakes of the cylindrical and NACA0012 towers during the passage of the rotor blade (from Janaireh et al.[11]). Note that the inscribed diameter was reduced for the aerodynamic shape which may reduce structural stiffness of the enclosed tower.

The researchers observed that the airfoil shaped tower produced a confined wake compared to the circular towers, and had the least overall impact on rotor instability. Figure 4 shows the wake of the circular and NACA0012 cross-section towers during the passage of the rotor. It is evident that the airfoil shaped tower has a significantly smaller wake and thereby has less of an impact on the blade.

C. Objectives

The primary objective of this study is to develop an aerodynamic shroud for a wind turbine tower to reduce the effects that the tower has on the rotor. This objective is accomplished by meeting several constraints. The velocity deficit in the wake is directly related to the tower drag, thus the shroud is designed to have the minimum drag possible. The shroud must inscribe a circular cylinder, preferably centered at the maximum thickness location to ensure that the shroud can fit around the tower while maintaining the minimum possible thickness. It is important to make sure that the aerodynamic forces on the shroud result in the proper moment about the tower center to ensure that it self-aligns with the wind direction when exposed to a non-zero angle of attack. The shroud must display a smooth pressure distribution without any large adverse pressure gradients that can lead to separation. The shroud should have the minimum possible distance between the inscribed cylinder center and its trailing edge while still meeting the other objectives because it limits how far downstream the rotor must be located thus reducing the cantilever loads that the tower must support.

II. Computational Methods – XFOIL

The shroud geometries were analyzed using XFOIL,[12] an open-source program for the design and analysis of subsonic airfoils, to analyze various shroud configurations. The program was used to determine the drag, moment, and pressure distribution for each airfoil in order to find an airfoil that best meets all of the above requirements. The initial design for the tower shroud was developed using XFOIL, which allows for both inviscid and viscous analysis. Only viscous results are presented in this paper. XFOIL is able to predict the pressure distribution around an airfoil at a given Reynolds number and angle of attack. It then uses the pressure data to calculate the lift, drag, and moment on the airfoil. XFOIL also enables the user to choose between free and forced transition. If forced transition is chosen the user is asked to specify a fixed location for transition to occur. This option is particularly useful when the boundary layer is forced to transition at a specific location on the real airfoil, i.e., placing a trip-strip on the airfoil. If free transition is used, the program will predict the location along the airfoil where boundary layer transition will occur.

For a given Reynolds number, XFOIL provides the drag coefficient based on the chord length of the airfoil (Eq. 1). For this study we are interested in the drag coefficient based on the tower diameter (Eq. 2), because the tower diameter is constant, and this will allow for a fair comparison in drag.

XFOIL has become a standard for the analysis of airfoils in incompressible flow but checks were still done to validate the data acquired from the program. The NACA0012 airfoil was used due to the large amount of experimental data available for it.

Figure 5 shows the drag polars at $Re = 3\text{x}10^6$ and $Re = 9\text{x}10^6$ (Eq. 3). The experimental data for both cases come from Abbott and von Doenhoff.[13] In both cases it can be seen that for the free transition case XFOIL follows the same trend as the experimental data, though it slightly underpredicts the drag coefficient. This underprediction can be compensated for if the correct transition location is known.

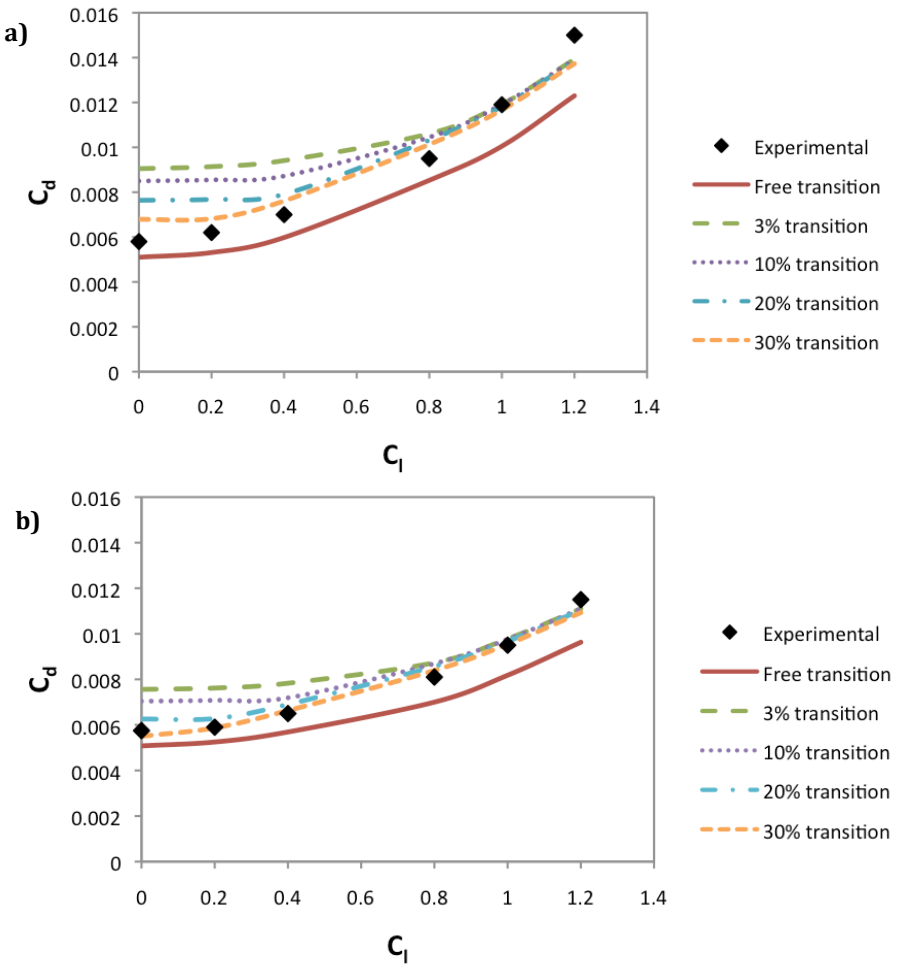

Figure 5. Drag polar of a NACA0012 airfoil comparing experimental data and XFOIL predictions for: a) Re=3x10^6 and b) Re=9x10^6 (experimental data from Abbott and von Doenhoff[13]).

The relationship between drag coefficient and Reynolds number is shown in Fig. 6. The experimental data for the 18% thick airfoil were taken from Blevins[9] while the computational data were determined using XFOIL. The change from a linear slope occurs due to the transition of the boundary layer from laminar-to-turbulent flow. For the free transition case, the XFOIL data seems to follow the same trend but slightly underpredicts the drag. Both the 3% and 20% transition cases follow the general trend, but they do not have the same shape where the boundary layer transition occurs, which is expected because the transition has already been forced at the lower Reynolds numbers.

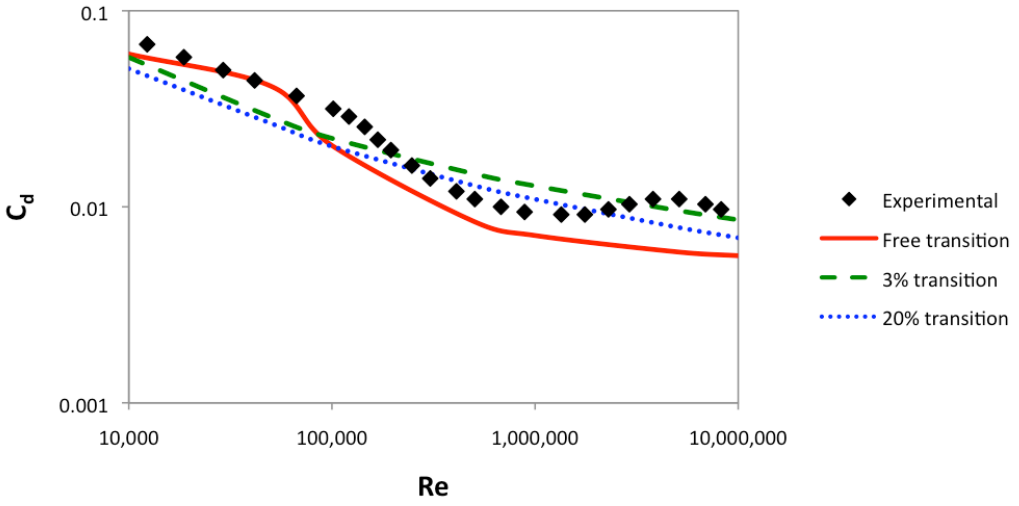

Figure 6. Drag as a function of Reynolds number of an 18% thick airfoil for experimental and computational cases (experimental data from Blevins[9]).

Overall, the validation showed that in general XFOIL is fairly accurate at predicting the aerodynamic forces on an airfoil, and experimental tests can be run to verify the data. In the case of the drag coefficient, where XFOIL tends to underpredict the drag when using free transition, the results are still useful for comparing airfoils because the trend is likely to be consistent for all airfoils considered in this study.

III. Shroud Design

A. Performance Objectives

As mentioned earlier, the shroud needs to meet several requirements in order to be suitable for use with a wind turbine tower. To reiterate, the shroud should have:

1) low drag, i.e., minimum $C_{d,D}$
2) self-aligning about cylinder center i.e., $C_{m_{\alpha D}} < 0$ about x_D
3) avoid strong adverse pressure gradients, i.e., C_p does not reduce drastically with x/c
4) short trailing edge i.e., minimum $x_{TE} - x_D$

Minimizing the drag is directly related to minimizing the wake effects of the tower. A negative $C_{m_{\alpha D}}$ will ensure that the shroud will self-align when subjected to a non-zero angle of attack. Having a reasonable pressure distribution means that the shroud should not experience any large adverse pressure gradients that can lead to flow separation at low angles of attack. Minimizing the distance between the tower center and the trailing edge of the shroud reduces the distance that the turbine rotor must be shifted downstream, thereby reducing the cantilever loads that the tower must be able to support.

B. Baseline Shroud Geometry

XFOIL was used to design the initial shroud geometry, in part by analyzing the drag of various symmetrical airfoils at zero angle of attack. The first step was to determine if it would be better to use a shroud with an elliptic cross-section or one with a typical symmetric airfoil shape. As seen earlier in Fig. 3, the drag coefficient is lower for symmetric NACA airfoils than for the elliptic shapes. From these results it was determined that a symmetric NACA airfoil would be selected for the baseline geometry, rather than an ellipse.

The next step was to determine which chord-to-thickness ratio would result in the lowest drag. The highly streamlined, thin airfoils (i.e., NACA0012) have less pressure drag than thicker airfoils (i.e., NACA0040), but they also have a longer chord length because the thickness is constant, which results in a higher skin-friction drag. XFOIL was used to help determine where the combination of pressure and skin-friction drag is minimized. Figure 7 shows the results at the Reynolds number for the full-scale tower, $Re_D = 8.3 \times 10^6$. The full-scale calculations use a wind speed of 12.5 m/s and a tower diameter of 10 m.

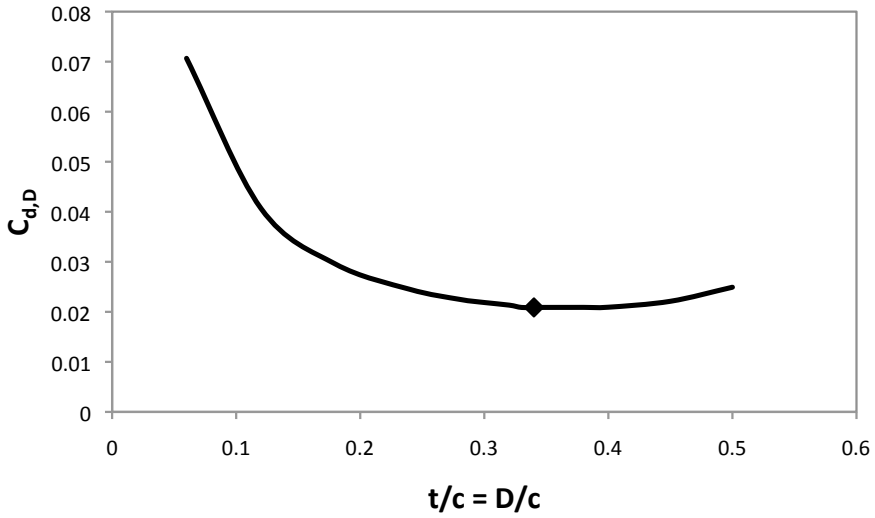

Figure 7. Drag coefficient as a function of thickness-to-chord ratio for symmetric NACA airfoils at $Re_D = 8.3x10^6$.

The results indicate that a three-to-one chord-to-thickness ratio results in the lowest drag. For this reason, the shrouds were designed to have a 33% thickness ratio. It should also be noted from Fig. 7 that there is not a significant increase in the drag for airfoils with a slightly higher or lower chord-to-thickness ratio. The baseline geometry was chosen to be a NACA0033 airfoil with the tower center located at the maximum thickness of the airfoil, which occurs at 30% of the chord, as shown in Fig. 2.

Based on the results from XFOIL, the NACA0033 has a positive $C_{m_{\alpha D}}$ (Eq. 5) about the tower center location and therefore is statically unstable, i.e. not self-correcting. If the flow approaches at a non-zero angle of attack, the shroud will be further misaligned resulting in a large increase in the drag and increasing the effects of the tower wake on the turbine blades. It was expected that the NACA0033 would not self-align because the tower center is located behind the quarter chord, which is typically where aerodynamic center is located for a thin symmetric airfoil.

C. Simple Cuff

In an attempt to create a shroud with minimum drag and a negative $C_{m_{\alpha D}}$ about the tower center, a series of new 33% thick airfoils was developed where the maximum thickness locations were further forward along the airfoil. The new airfoils were created by starting from a NACA0028, NACA0030 and NACA0031, all three of which have the maximum thickness located at 30% of chord. The front end of each airfoil was then trimmed so that the leading edge of the airfoil was a cylinder centered about the maximum thickness location. By making this change the new geometry has the maximum thickness located much closer to the leading edge thereby increasing the change that the shroud will have a negative $C_{m_{\alpha D}}$ about the inscribed cylinder center. Figure 8a shows a schematic of a NACA0031 airfoil with the front trimmed to a cylinder.

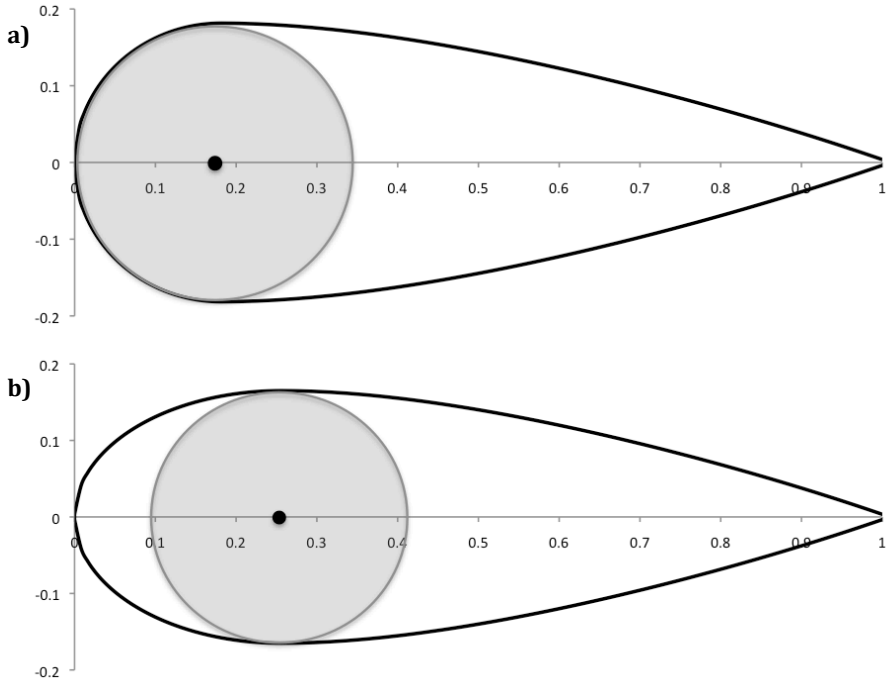

Figure 8. Schematic of a NACA0031 airfoil with the front end replaced with a semi-cylinder: a) with no cuff yielding 36.3% *D/c* and b) with a cuff based on 33% *D/c*.

The new airfoil geometry has a blunted leading edge and a chord-to-thickness ratio greater than the optimal 33%, both of which lead to an increase in drag. This problem was remedied by adding a leading-edge cuff to each airfoil to yield a 33% thickness ratio while also reducing the bluntness. The distribution of the cuff shape varied linearly from a set length at the leading edge to zero at the maximum thickness location. Various cuff shapes were explored but a linear distribution was found to be the simplest and most effective shape. The airfoil with the cylindrical front that originated from the NACA0031 required a cuff that was 10% of its chord length to achieve a 33% thick airfoil. The airfoils that originated from the NACA0028 and NACA0030 required cuffs that were 1.15% and 7.1% of their chord lengths respectively. The three airfoils of the new 'simple cuff' series were named the C28, C30 and C31 where the C stands for 'cuff' and the symmetric NACA airfoil it originated from is represented by the number. A schematic of the newly developed C31 airfoil is shown in Fig. 8b.

The drag coefficient and moment coefficient were found using XFOIL for the full scale Reynolds number of each airfoil based on a thickness of ten meters. The results show a tradeoff between the drag and pitching moment. The C31 has the lowest drag of the new airfoils but it also has a slightly positive $C_{m_{\alpha D}}$. On the other hand, the C28 has the best $C_{m_{\alpha D}}$ but it also has the highest drag. The C30 airfoil seems to meet the objectives the best out of all the airfoils.

A third objective in developing the shroud is to have a smooth pressure distribution without any large adverse pressure gradients. Figure 9 shows the pressure distribution along each airfoil at a zero degree angle of attack. It can be seen that all of the new airfoils have a sudden drop in the pressure around their maximum thickness location. This large adverse pressure gradient can lead to separation, which would greatly increase both the drag of the shroud and the turbulence of the wake. The adverse pressure gradient is particularly bad for the C28 airfoil as the pressure drop is nearly vertical at one point.

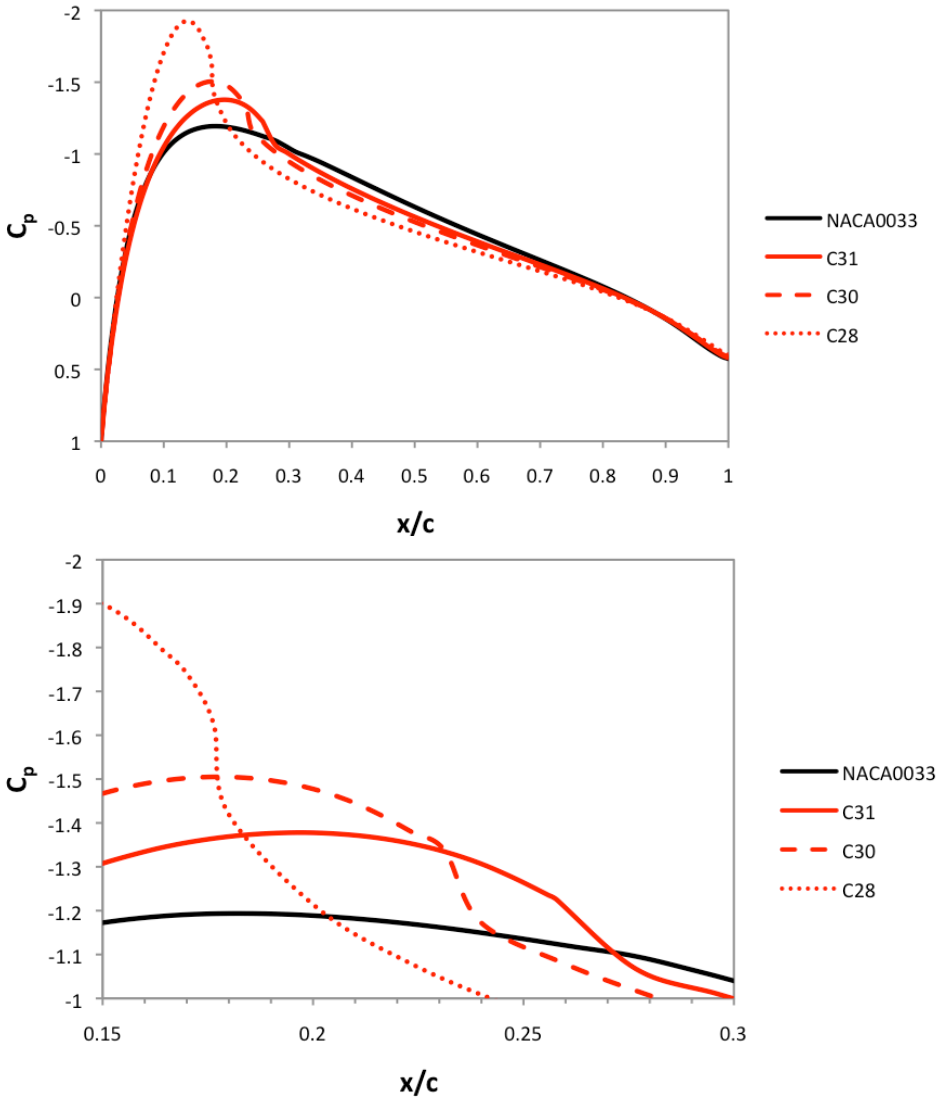

Figure 9. Pressure distribution for the NACA0033, C31, C30 and C28 airfoils at zero degree angle of attack.

D. Advanced Design

Slightly varying the geometry of each airfoil can help to smooth the pressure gradient without significantly affecting the drag or moment. The new airfoils were designed using PROFOIL,[14] which is an inverse design method that allows for the prescription of the desired velocity distribution from which the geometry is determined. The method was applied for each case with and without the constraint that the slope must be near zero at the original maximum thickness location, resulting in six new airfoils to go along with the three originals. The airfoils that were created with the constraint are designated with a 'c' in the airfoil name, e.g., C31c, and are referred to as the 'constrained' series. The airfoils that were created without the constraint are designated with a 'u', e.g., C31u, and are referred to as the 'unconstrained' series.

There are two options on how to handle the airfoils without the zero slope constraint. The first is to leave the tower at the original maximum thickness location, which will result in a thicker airfoil with increased drag, but the moment should not be affected significantly. The second option is to place the tower at the new maximum thickness location which will result in a lower drag because of the smaller absolute thickness, but it would have poorer $C_{m_{\alpha_D}}$ characteristics because the tower center is farther aft on the

airfoil. The two options were distinguished by adding a 's' for the case where the tower location is shifted to the new maximum thickness, e.g. C31us. The C28us, C30us, and C31us airfoils are referred to as the 'unconstrained-shifted' series. A breakdown of the properties of each shroud design is shown in Table 1.

Table 1. Shroud properties for 15 MW wind turbine with D = 10 m

Airfoil	t/c	t/D	x_D	x_t	$C_{d,D}$	$C_{m_{\alpha}D}$	$x_{TE} - x_D$
NACA0033	0.330	1	0.301	0.301	0.0210	0.00828	0.699
C31	0.330	1	0.256	0.256	0.0213	0.00172	0.744
C31c	0.330	1.000	0.256	0.253	0.0218	0.00562	0.744
C31u	0.333	1.007	0.256	0.284	0.0187	0.00066	0.744
C31us	0.333	1	0.284	0.284	0.0186	0.00376	0.716
C30	0.330	1	0.231	0.231	0.0222	-0.00224	0.769
C30c	0.330	1.000	0.231	0.225	0.0210	-0.00040	0.769
C30u	0.336	1.013	0.231	0.279	0.0193	-0.00256	0.769
C30us	0.336	1	0.279	0.279	0.0191	0.00290	0.721
C28	0.330	1	0.176	0.176	0.0234	-0.00876	0.824
C28c	0.331	1.001	0.176	0.196	0.0237	-0.00260	0.824
C28u	0.355	1.034	0.176	0.248	0.0217	-0.00406	0.824
C28us	0.355	1	0.248	0.248	0.0211	0.00296	0.752

The drag coefficient and $C_{m_{\alpha}D}$ results for all airfoils are presented in Fig.10 as well as in Table 1. The C31us had the minimum drag, but it had a positive $C_{m_{\alpha}D}$ value. The C28 had the best pitching moment performance, but it also had the second highest drag of all the airfoils. The C30u had the best overall performance in terms of drag and moment with the fourth lowest drag and the fourth lowest $C_{m_{\alpha}D}$ value. The unconstrained-shifted series had the best drag performance, with the unconstrained series a close second, while the simple cuff series and the unconstrained series performed the best with respect to the pitching moment. The unconstrained series had the best balance between the drag and moment. Coordinates for the unconstrained series airfoils are given in the appendix.

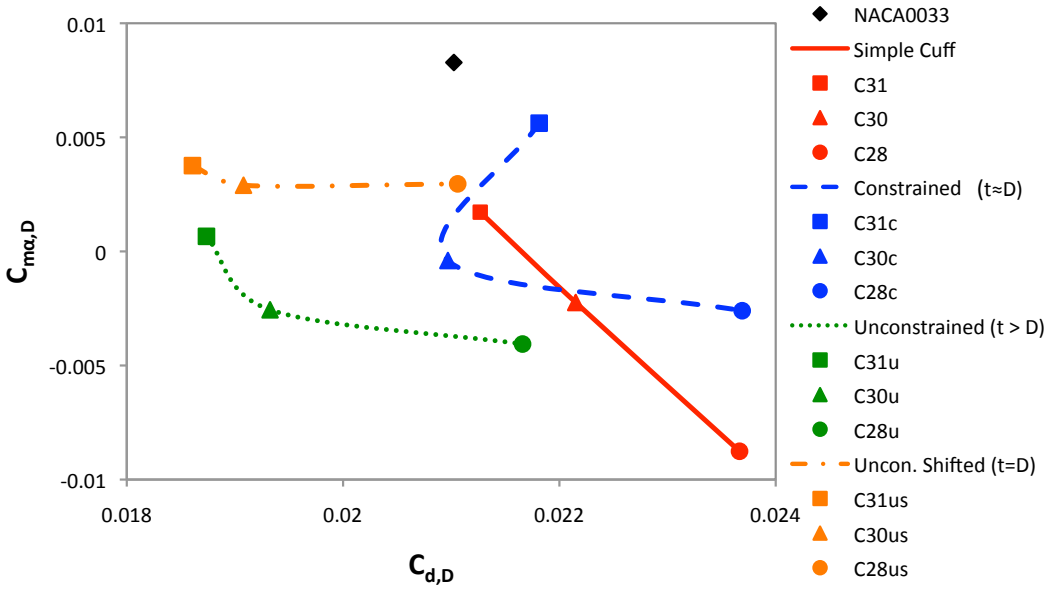

Figure 10. Drag and pitching moment coefficients for Re_D = 8.3x10^6 (based on D = 10 m and V = 12.5 m/s).

Figure 11 shows the pressure distributions at zero degree angle of attack for the unconstrained series. There was a significant improvement in the pressure distribution when compared with the simple cuff series (Fig. 9) as none of the airfoils experienced a large adverse pressure gradient. The C28u had the highest peak in C_p but it was still an improvement from the C28.

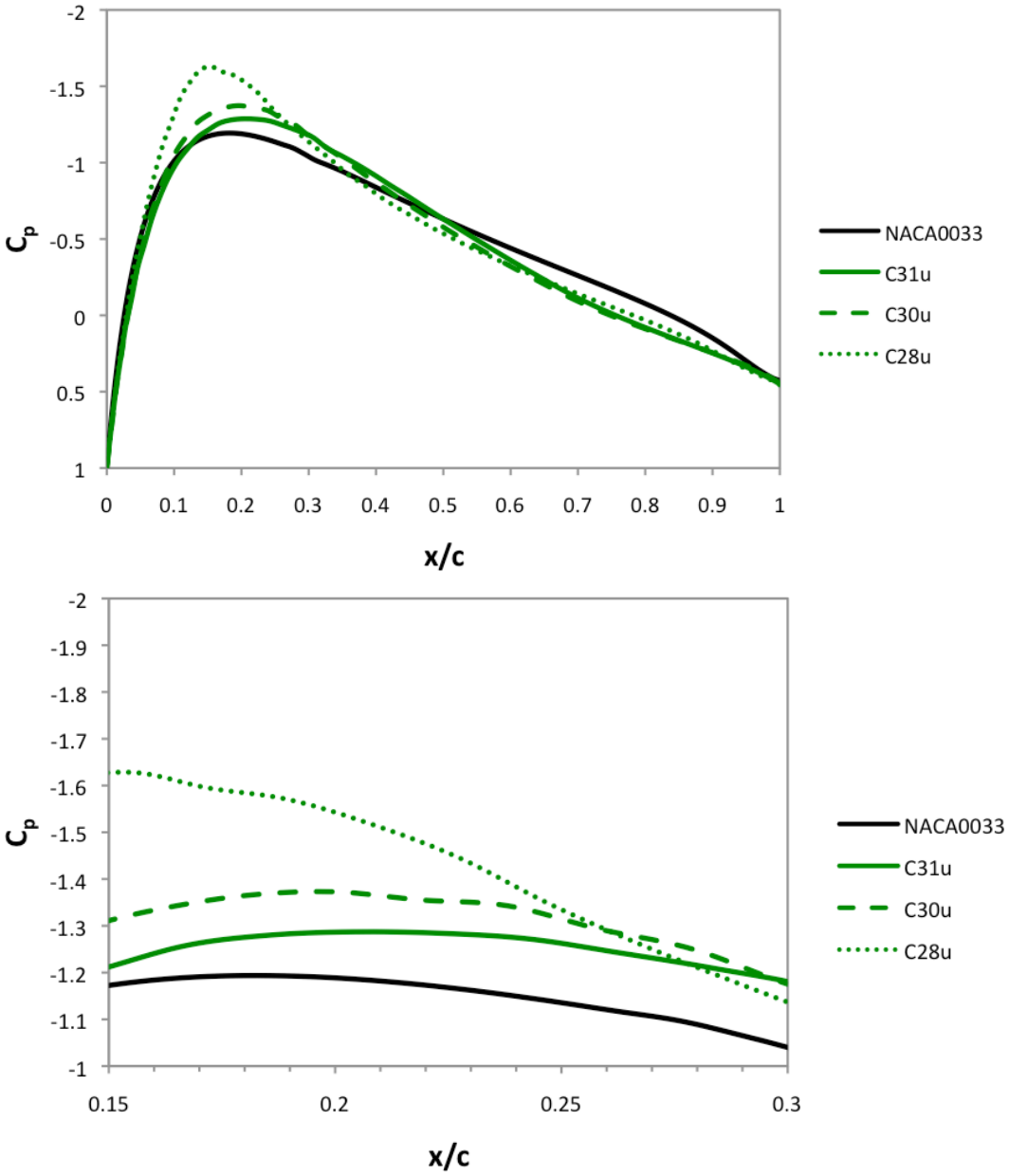

Figure 11. Pressure distribution for the "unconstrained" airfoils at zero degree angle of attack.

The C30u performed the best with respect to the drag and pitching moment and also had a well-behaved pressure distribution. The airfoil was designed to inscribe a cylinder, and if the cylinder center were located farther back along the airfoil then the $C_{m_{\alpha,D}}$ value would have suffered. The C30u met all of the performance objectives and was thereby chosen as the best geometry for the tower shroud.

IV. Conclusions

The methods discussed above were used to develop a range of possible designs for the tower shroud. Analysis of the designs was performed using XFOIL. A three-to-one chord-to-thickness ratio was determined to result in the minimum tower drag. The baseline design was chosen to be a NACA0033 airfoil, but it had a positive $C_{m_{\alpha D}}$ value. A NACA0028, NACA0030, and NACA0031 airfoil were each modified with a simple cuff design to give them a 33% thickness ratio. The resulting airfoils all experienced a significant adverse pressure gradient that could lead to flow separation. PROFOIL was used to adjust the airfoil geometry so that the pressure distribution was well behaved. The program was run with and without a constraint on the slope of the airfoil at the inscribed cylinder center location. This method produced two new airfoil families and shifting the tower location to the new maximum thickness for the unconstrained family created a third. Of the three new series of airfoils, the unconstrained series performed the best. The C30u design had the best balance between drag and moment performance with a $C_{d,D}$ value of 0.0193 and a $C_{m_{\alpha D}}$ value of -0.00256 at Re_D = 8.3x10^6, and it also had a well-behaved pressure distribution. The drag of the C30u is only 2.5% of the drag for a cylinder at the same Reynolds number. The C30u was determined to be the best design for the tower shroud.

The next step is to test the designs experimentally. A model of the tower shroud can be made using 3-D printers available at the University of Virginia (UVA), and the experiments will be run in a water tunnel that is also at UVA. A test will be run to simulate the effects of a blade passing through the wake. A model of the turbine blade will be weighted and released in the water tunnel behind the shroud, and the change in velocity when passing through the wake will be recorded. From the results, the size of the wake velocity deficit can be found.

Appendix

C28u		C30u		C31u	
x/c	*y/c*	*x/c*	*y/c*	*x/c*	*y/c*
1.0000000	0.0000000	1.0000000	0.0000000	1.0000000	0.0000000
0.9943823	0.0011923	0.9948056	0.0010140	0.9947505	0.0010415
0.9795963	0.0049851	0.9809034	0.0040659	0.9807339	0.0042025
0.9573099	0.0113276	0.9595062	0.0090626	0.9592171	0.0094071
0.9286984	0.0200634	0.9313959	0.0159461	0.9310326	0.0166107
0.8947939	0.0307625	0.8972714	0.0247607	0.8969536	0.0258248
0.8562668	0.0428623	0.8580381	0.0354539	0.8578995	0.0369320
0.8136837	0.0560404	0.8145958	0.0478298	0.8147605	0.0496957
0.7677072	0.0700044	0.7685724	0.0616068	0.7684362	0.0638063
0.7190131	0.0844454	0.7187472	0.0764022	0.7198389	0.0788570
0.6683184	0.0990539	0.6681734	0.0917164	0.6698599	0.0943254
0.6163671	0.1134243	0.6169549	0.1068525	0.6193051	0.1094965
0.5637640	0.1271743	0.5655644	0.1211950	0.5686334	0.1237028
0.5111635	0.1399602	0.5145026	0.1342661	0.5182628	0.1364502
0.4591872	0.1514224	0.464200	0.1456643	0.4685834	0.1473312
0.4084187	0.1612137	0.4151177	0.1550349	0.4199607	0.1560158
0.3594045	0.1690032	0.3676470	0.1620542	0.3727399	0.1622453
0.3126481	0.1744600	0.3221481	0.1664499	0.3272476	0.1658216
0.2685603	0.1772638	0.2789119	0.1679837	0.2837758	0.1666022
0.2274531	0.1771686	0.2381180	0.1665286	0.2425675	0.1645278
0.1896152	0.1739389	0.1999508	0.1620843	0.2038599	0.1596288
0.1551107	0.1674318	0.1645799	0.1547422	0.1678865	0.1520017
0.1240728	0.1576277	0.1322111	0.1446582	0.1348749	0.1417996
0.0962649	0.1445719	0.1030148	0.1320195	0.1050460	0.1292245
0.0716616	0.1287397	0.0771386	0.1170827	0.0786161	0.1145058
0.0503976	0.1105965	0.0547277	0.1001640	0.0557437	0.0979030
0.0326362	0.0905754	0.0359248	0.0816238	0.0365678	0.0797475
0.0185471	0.0691151	0.0208695	0.0618619	0.0212275	0.0604215
0.0083491	0.0466326	0.0097052	0.0413208	0.0098703	0.0403481
0.0021431	0.0234386	0.0026181	0.0204964	0.0026658	0.0199993
0.0000000	-0.0000005	0.0000000	0.0000000	0.0000000	0.0000000

References

[1]Loth, E., Selig, M.S., and Moriarty, P., "Morphing Segmented Wind Turbine Concept," *AIAA Applied Aerodynamics Conference*, AIAA-2010-4400, Chicago, IL, June 2010.

[2]Loth, E., Steele, A., Ichter, B., Selig, M.S., and Moriarty, P., "Segmented Ultralight Pre-Aligned Rotor for Extreme-Scale Wind Turbines," *AIAA Aerospace Sciences Meeting*, AIAA-2012-1290, Nashville, TN, Jan. 2012.

[3]Ichter, B., Steele, A., Loth, E., and Moriarty, P., "Structural Design and Analysis of a Segmented Ultralight Morphing Rotor (SUMR) for Extreme-Scale Wind Turbines," *AIAA Fluid Dynamics Conference*, AIAA-2012-3270, New Orleans, LA, June 2012.

[4]Lee, S.J., Lee, S.I., and Park, C.W., "Reducing the Drag on a Circular Cylinder by Upstream Installation of a Small Control Rod," *Fluid Dynamics Research*, Vol. 34, No. 4, Apr. 2004, pp. 233-250.

[5]Mashud, M., Islam, M.S., Bari, G.S., and Islam, M.R., "Reduction of Drag Force for a Cylinder by Attaching Cylindrical Rings," *Asian Congress of Fluid Mechanics*, Dhaka, Bangladesh, Dec. 2010, pp. 174-177.

[6]Sosa, R., D'Adamo, J., and Artana, G., "Circular Cylinder Drag Reduction by Three-Electrode Plasma Actuators," *Journal of Physics: Conference Series*, Vol. 166, No. 1, 2009.

[7]Hwang, J.Y., Yang, K.S., "Drag Reduction on a Circular Cylinder Using Dual Detached Splitter Plates," *Journal of Wind Engineering and Industrial Aerodynamics*, Vol. 95, No. 7, July 2007, pp. 551-564.

[8]Triyogi, Y., Suprayogi, D., and Spirda, E., "Reducing the Drag on a Circular Cylinder by Upstream Installation of an I-type Bluff Body as Passive Control," *Journal of Mechanical Engineering Science*, Vol. 223, Oct. 2009, pp. 2291-2296.
[9]Blevins, R., *Applied Fluid Dynamics Handbook*, Van Nostrand Reinhold Company Inc., New York, 1984.
[10]Hand, M., Simms, D., Fingersh, L.J., et al., "Unsteady Aerodynamics Experiment Phase VI: Wind Tunnel Test Configurations and Available Data Campaigns," NREL/TP-500-29955, Dec. 2001.
[11]Janajreh, I., Talab, I., and Macpherson, J., "Numerical Simulation of Tower Rotor Interaction for Downwind Wind Turbine," *Modelling and Simulation in Engineering*, 2010.
[12]Drela, M., "XFOIL: An Analysis and Design System for Low Reynolds Number Airfoils," *Conference on Low Reynolds Number Airfoil Aerodynamics*, University of Notre Dame, June 1989.
[13]Abbott, I. and von Doenhoff, A., *Theory of Wing Sections: Including a Summary of Airfoil Data*, New York: Dover Publications, 1959.
[14]Selig, M.S. and Maughmer, M.D., "Generalized Multipoint Inverse Airfoil Design," *AIAA Journal*, Vol. 30, No.11, Nov. 1992, pp. 2618-2625.